THE PROCESSING OF CASI-1500I DATA AT INTA PAF

Eduardo de Miguel[1], Alix Fernández-Renau[1], Elena Prado[1], Marcos Jiménez[1], Óscar Gutiérrez de la Cámara[1], Clara Linés[1], José Antonio Gómez[1], Ana I. Martín[2] and Félix Muñoz[2]

1. INTA, Torrejón de Ardoz, Spain; demiguel(at)inta.es
2. ISDEFE, Madrid, Spain

ABSTRACT

The Remote Sensing Laboratory at INTA has been operating a CASI-1500 instrument since 2009. A specific processing chain has been implemented within the INTA airborne data Processing and Archiving Facility. In this chain, raw data (level 0 product) are transformed to at-sensor radiance (level 1b) and later to geolocated at-sensor radiance (level 1c). Other processing levels, as atmospherically corrected reflectance (L2b / L2c), can also be produced. The resulting image products are delivered together with radiometric statistics, metadata and quality descriptors, the latter according to EUFAR HyQuaPro recommendations. In this paper, details about this processing chain are given, including some points related to in-flight spectral calibration and noise and SNR estimation in operational images. The paper also describes the procedure for in-flight geometric calibration (internal orientation calibration and boresight estimation). Finally, an evaluation of the products accuracy (radiometric, spectral and geometric) is presented, using imagery from CASI campaigns performed by INTA.

INTRODUCTION

CASI is a well-known series of visible to near-infrared airborne imaging spectroradiometers, developed and commercialized by Itres (Ontario, Canada). The remote sensing laboratory at INTA has been operating a CASI-1500i since 2009 in different remote sensing projects. Together with the calibration and navigation equipment, auxiliary ground instrumentation and a specific Processing and Archiving Facility (PAF), it forms the INTA CASI system. INTA offers this system as a technological service to public institutions or commercial companies, having performed over 25 flight campaigns since 2009. In this paper, this system is described, focusing on its PAF. A twin system, based on the AHS 80-band imaging radiometer, is also available, with both instruments nominally used in a tandem configuration. The corresponding INTA AHS PAF is presented in a separate paper (1).

The CASI 1500i instrument

The CASI 1500i is a pushbroom imager based on a two-dimensional CCD; the instrument measures the incoming radiance along up to 1500 spatial pixels "across-track" in up to 288 separate spectral bands. The spectral bands can be placed anywhere within the CASI 380 to 1050 nm spectral range. The band-to-band distance between spectral rows is 2.4 nm, while the bandwidth of each spectral row is around 3 nm. Each (#spatial $\times$ #spectral) array of pixels acquired simultaneously is sometimes called a frame. Incoming radiation is stored in 14 bits per sample.

The 1500 pixels across track are reduced to 1440 if the so-called spectral mode is selected. In this mode, the read-out of the CCD spectral dimension can be performed with different binning factors (or *row-sums*), reducing the spectral resolution to increase the signal-to-noise ratio. In the alternative spatial mode, in which the 1500 spatial pixels are used, either the full spectral dimension or custom-defined subsets of bands (with different binnings per set) can be recorded.

With a total Field of View (FOV) of 40° and an Instantaneous FOV (IFOV) of 0.5 mrad, CASI provides an across-track spatial resolution 5 times better than the INTA AHS at the same flight altitude. The along-track pixel size is defined by the selected integration time. The signal-to-noise ratio

DOI: 10.12760/01-2014-1-04

(SNR) can be increased, while keeping a fairly square measurement, by selecting an integration time slightly above the one corresponding to the across-track pixel size.

Dark frames and uniformity frames are automatically recorded before and after each imaged scene using specific elements of a wheel mounted in front of the aperture. Dark frames are obtained by placing a shutter instead of the nominal slit, while uniformity frames (intended to detect an eventual contamination of the aperture slit) use an optical diffuser. Masked columns in the edges of the CCD are used to estimate electronic offset, while columns which are neither masked nor illuminated by the slit are used to estimate focal plane straylight.

The determination of absolute radiometric calibration coefficients is performed at INTA by illuminating the system with an integrating sphere from Sphere Optics (NH, USA), following the procedures defined by the instrument vendor. Dark frames are used to obtain the system output at zero input radiance. Considering also CCD smear and straylight, a linear model relating digital output to input radiance is built. This model is computed per pixel and per band, and the resulting coefficients stored in a calibration matrix.

For the spectral calibration, lamps of gases with specific emission peaks are used to locate bandcentres, again using the hardware and procedures defined by Itres. Spectral responsivity curves are not evaluated, but a Gaussian model is assumed.

The CASI sensor includes an integrated Applanix POS/AV direct georeferencing system. POS/AV includes a post-processing software suite called POSPac-MMS (2) to retrieve external orientation parameters. The synchronization of CASI-1500i and POS/AV measurements is performed by matching time measurements from both instruments. Geometric calibration is required to estimate the boresight angles, i.e. the angles between the POS/AV Inertial Measurement Unit (IMU) axis and sensor (image) axis. The IMU is fixed to the sensor body, but its reference system is slightly rotated with respect to the sensor (and image) coordinate system. This requires the relation of both reference systems to be determined in terms of roll, pitch and yaw misalignments. The boresight angles are computed through a bundle adjustment implemented in the Itres software tool *pbsbund*. The input to *pbsbund* is an extensive set of Ground Control Points (GCPs) collected at a calibration field over which a pattern of crossing and overlapping flight lines is flown. A differential GPS field campaign is performed to collect cartographic coordinates of these GCPs. The estimated boresight angles are valid as long as the sensor / IMU / GPS locations do not change their relative positions, and therefore for a complete flight season, as reported for other sensors (3).

INTA CASI products

The INTA Remote Sensing Laboratory performs the processing of the images acquired with the CASI. Different processing level products are available to the users, following the classical categories L1a, L1b, L1c, L2b and L2c. Table 1 defines each possible product.

Table 1. INTA-CASI products.

Level 1 image product	L1a	**Raw product:** digital numbers recorded by CASI. No radiometric calibration or signal correction applied. Geomatica "pix" format instead of the native recording format.
	L1b	**User product:** georeferenceable at sensor radiance in BSQ format + ENVI header, with Input Geometry Data (IGM file) for image geometric correction + QA products.
	L1c	**User product:** georeferenced at sensor radiance BSQ format + ENVI header + QA products.
Level 2 image product	L2b	**User product**: georeferenceable hemispherical-directional reflectance factor BSQ format + ENVI header, usually with Input Geometry Data (IGM) for image geometric correction.
	L2c	**User product:** georeferenced hemispherical-directional reflectance factor BSQ format + ENVI header.

DESCRIPTION OF THE PROCESSING CHAIN

In the INTA-CASI PAF, in-house developed tools (based mainly in shell scripts and IDL) and some pieces of commercial software are integrated in an operational workflow. The integration is not designed for a fully automatic operation, but rather for a modular use: each step in the workflow must be configured manually and launched by an operator, and then runs alone for the specified dataset. Figure 1 presents an overview of the INTA-CASI PAF operational flow; details are given in the following sections.

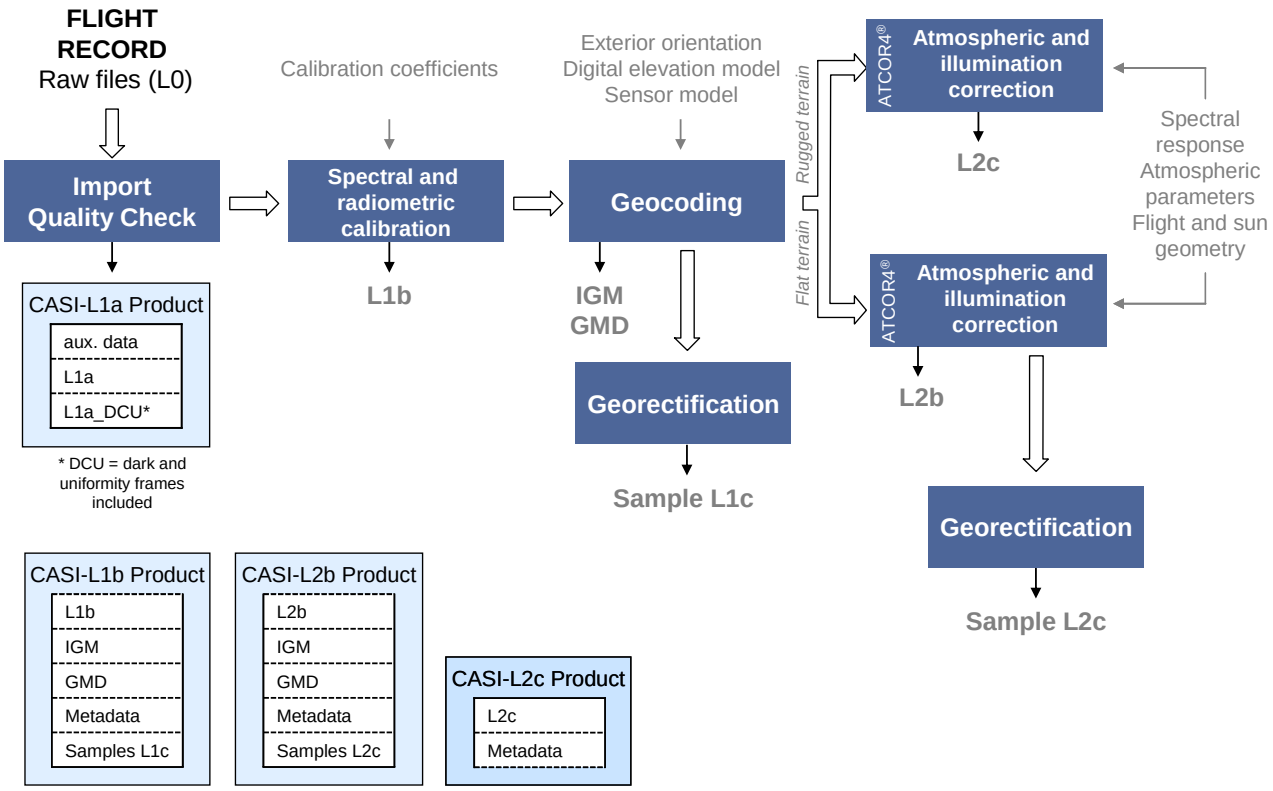

Figure 1: Overview of the INTA-CASI PAF operational workflow.

Radiometric calibration

Image radiometric calibration is performed with the Itres tool *radcorr*. It transforms the image values from digital number to at-sensor radiance (Ls) for VNIR region, according to a two-step linear model. First, the raw digital number is corrected subtracting additive non-signal terms.

$$DN_{i,j,k} = DN0_{i,j,k} - DC_k - ISL_{i,k} - FSS_{i,k} - EO_{i,k}$$

where the subscripts {*i*,*j*,*k*} correspond to image {row, column, band} respectively; $DN_{i,j,k}$ is the corrected but uncalibrated signal; $DN0_{i,j,k}$ is the raw signal; DC_k is the average dark current for band *k*, as measured just before image acquisition; $ISL_{i,k}$ is the internally scattered light, *FSS* is frame shift smear, and $EO_{i,k}$ is the electronic offset. *ISL*, *FSS* and *EO* are estimated according to Itres recommendations using CCD information. Note that a detector element outside the slit image is used for straylight estimation per band, recording photons originated anywhere in the focal plane, and therefore from any wavelength (i.e., spectral straylight). Of course, this approach does not account for an eventual uneven pattern of straylight across the CCD spatial dimension.

Next, the corrected digital number is calibrated to at-sensor radiance by means of laboratory coefficients.

$$Ls_{i,j,k} = \frac{1}{sc_{i,j,k}} DN_{i,j,k}$$

Here, *sc* is the calibration coefficient as computed in the laboratory calibration using Itres software *sparcal*. The *radcorr* tool adjusts automatically to account for the eventual spectral binning factor applied during image acquisition.

Note that this two-step procedure represents a linear model where the slope depends on laboratory measurements, but the offset is estimated from the actual image.

By selecting the right *radcorr* configuration, it is possible to obtain intermediate products, such as:

- uncorrected and uncalibrated images, i.e. the L1a product in Table 1, useful only to researchers who would like to work from the raw image data, which is only delivered on request,
- corrected but uncalibrated images, which are used for calibration analysis,
- either full-frame files, i.e. including dark-current and uniformity frames, or image-frames-only files.

Geolocation and IGM

The geolocation of airborne linescanner data based on direct georeferencing technique requires an accurate determination of the position and attitude of the scanning instrument. These parameters are derived from the continuous acquisition data with combined GPS and IMU measurements.

The geolocation of each CASI pixel is performed from the exterior orientation information, the digital elevation model (DEM) and a detailed sensor model, using the *geocor* tool provided by Itres. The basic output of the process is an input geometry file (IGM) for each image. IGM image files denote the UTM easting and northing values derived by the geolocation process for each original image pixel. The IGM files have the same spatial size as the CASI L1b imagery and contain the geolocation information for each original pixel.

Resampling

The CASI orthorectified data cube can be created in different ways depending on the resampling algorithm used. In our nominal processing chain we use the *geocor* tool, applied only to a subset of visible bands (allowing either a true colour or infrared colour composite). These georectified bands are delivered to the user mainly as a quicklook to display the expected output of the orthorectification process. Users are expected to choose their own resampling algorithm to produce the complete orthorectified data cube from the delivered IGM with the support of that georectified quicklook.

A specific problem is the selection of the output pixel size during resampling. The reason is that, in some cases, the integration time selected for the image acquisition defines an along-track pixel size which is significantly above the across-track pixel size defined by the instrument IFOV. In such cases, resampling to a square grid must consider a compromise between redundancy (original samples that are used more than once when generating the resampled product) and data loss (raw original samples that are not mapped to the resampled product). A dedicated analysis is presented in (4).The value used in the INTA PAF for the georectified quicklook is intended to optimize this compromise, and users are recommended to apply this value.

L2 products

Atmospheric and illumination correction is performed with ATCOR4 (5), which is a LUT-based implementation of MODTRAN5 targeted for airborne remote sensing data. Following the definitions in (6), the magnitude estimated by ATCOR4 is the Hemispherical-Directional Reflectance Factor (HDRF) of the observed surface.

For the ATCOR4 configuration, atmospheric water vapour is estimated using the depth of the 940 nm water vapour absorption feature. Visibility and aerosol type are estimated either from external atmospheric data or using the ATCOR4 algorithm to estimate them from spectral statistics of pixels corresponding to dense-dark vegetation.

In specific campaigns, INTA acquires and processes ASD FieldSpec-3 spectra with the objective of supporting the generation of L2 products. These spectra could be used either as inputs to

ATCOR4, which includes functionalities for in-flight calibration and atmospheric parameters' fine-tuning, or as ground truth for validation of the obtained reflectance products.

Metadata and quality reporting

A first evaluation of the quality of acquired images is performed in near-real time during the flight campaign. This quick quality assessment is required to agree with the user on the successful completion of the planned flight programme.

Metadata elements and quality parameters for higher level products are generated following the recommendations given by the EUFAR-HyQuaPro activity (7). Accordingly, we systematically attach to each image product a text file with a pre-defined set of fields reporting image acquisition parameters and processing, lineage and contact information. This text file is generated by a specific shell script.

In addition to these quality descriptors, image statistics are computed per band and provided to the user in a specific text file. This statistics file contains saturated pixels count and scene average signal and noise.

Dark current is a thermally-generated, non-target related signal originating in the silicon structure of the CCD, and present even when the aperture is closed. During operations, the CCD is thermoelectrically cooled to reduce and stabilize its dark current noise. Dark current is recorded at the start and end of each recorded image file automatically. The dark current registered at the beginning of the flight line is then subtracted from the image signal during calibration.

A potential drift of the dark current during image acquisition is tracked by comparing the average dark current at the beginning and end of the flight line. If the difference between them is higher than a few *DN*, images are recalibrated to compensate for this drift in the dark current signal, before higher level processing or image delivery.

Uniformity data are also acquired both at the opening and closing of an image file. Uniformity frames are collected for use should contamination of the spectral slit (part of the lens assembly) be detected through examination of processed image files. These data can be regarded as a "snapshot" of the condition of the slit at the time that an image file was opened and again upon closure. Since these data are collected through an optical diffuser, they are only influenced by low frequency structure being, thus, a good candidate for instrumental noise assessment. After removal of the low frequency structure, the standard deviation of the radiometrically calibrated uniformity data is taken as an estimation of the CASI instrumental noise - *NEdL*. The *SNR* is given as the ratio of the mean signal of the image (radiometrically calibrated and excluding scene borders) to *NEdL*.

Finally, specific information is provided on the geometrical features of each pixel. These are the so-called geometric metadata (GMD), which are reported as layers in an auxiliary file, with the same pixel-column dimensions as the radiometric data, but with the following info as bands:

- View (scan) zenith angle.
- View absolute azimuth.
- Pixel distance (= view path length)
- Ellipsoidal terrain height
- Actual GIFOV across-track
- Actual GIFOV along-track

These values are computed following rigorous models and using actual flight, sensor and terrain information. This is an essential file to take into account during image analysis several effects that appear in airborne remote sensing imagery.

PRODUCTS QUALITY

Radiometric quality

A simple and generic evaluation of the radiometric accuracy of CASI radiometric measurements is not possible. It depends on a number of variables, among others the amount of operation hours since the applicable laboratory calibration and specific atmospheric conditions. An average 1-2% loss of sensitivity after a flight season has been evaluated in laboratory; this degradation appears uniformly along the spectral dimension.

The estimated radiometric accuracy for a specific dataset, along with other detailed system performance parameters (like or dark current variations) can be provided on request.

On the other hand, and as stated above, an estimation of noise and SNR for each image is performed systematically. Figure 2 shows results of *NEdL* for data acquired in 2012.

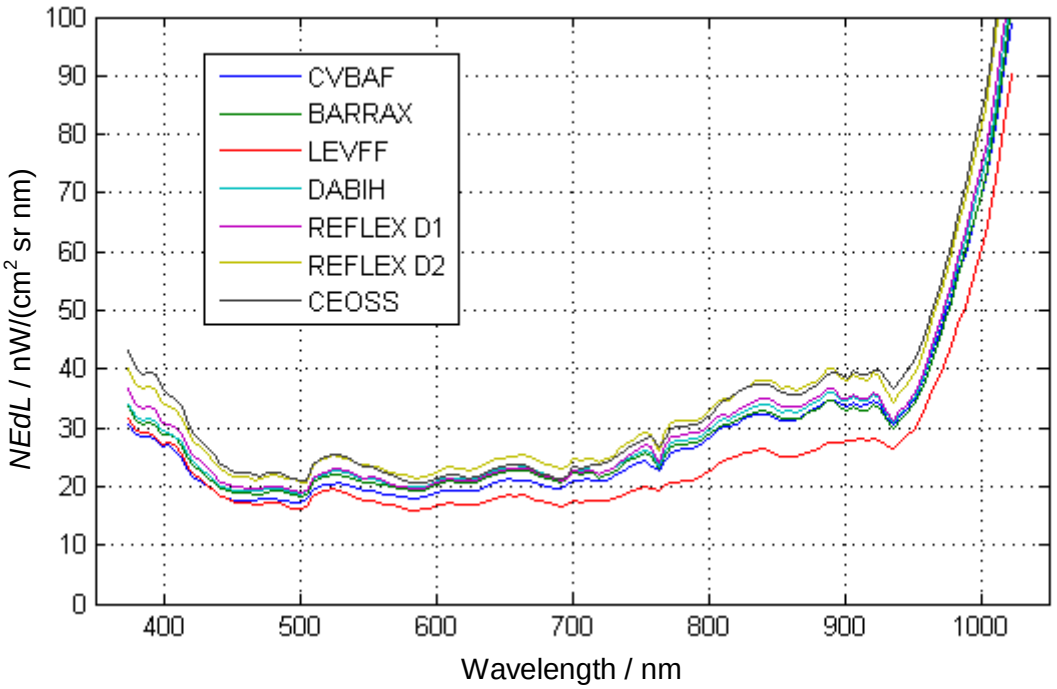

Figure 2: Estimated NEdL for INTA CASI 1500i images acquired in spectral mode "row sum 2" (i.e., spectral binning 2, which is the most used setting) during 2012. Each line represents the average of a flight session.

The figure shows that *NEdL* is always below 40 nW/(cm^2 sr nm) and usually below 30 nW/(cm^2 sr nm) for most of the bands. Only above 1000 nm, when responsivity of silicon detectors decreases severely, the *NEdL* increases significantly.

Spectral accuracy

The design of the CASI spectrometer limits the spectral smile to less than 1 spectral pixel. On the other hand, a minor spectral shift is expected as a result of environmental conditions during the flight. This means that there is a change in the effective band centre during image acquisition, when compared to the nominal (laboratory) band centre. A specific tool is provided by Itres to perform spectral-shift checks and correction in operational images. However, it only works on spatial mode, while the shift can be very significant and detectable in other CASI modes. Therefore, we have produced a specific tool, similar to those presented in (8,9,10). This tool maximizes the correlation between image *Ls* spectrum and MODTRAN generated *Ls* shifted spectra, in the band-A oxygen absorption region. The first step in the tool is to select oxygen band-A channels; a unique spectrum per image column is created. Next, a MODTRAN reference spectrum in the same spectral region is resampled to the image spectral configuration and shifted up to 5 nm NIR and toward

blue in steps of 0.1 nm. The best fit between the MODTRAN and observed spectra per column is chosen, and an image-specific CCD spectral map is created. This is the new input to the calibration procedure. An example of the results obtained is displayed in Figure 3.

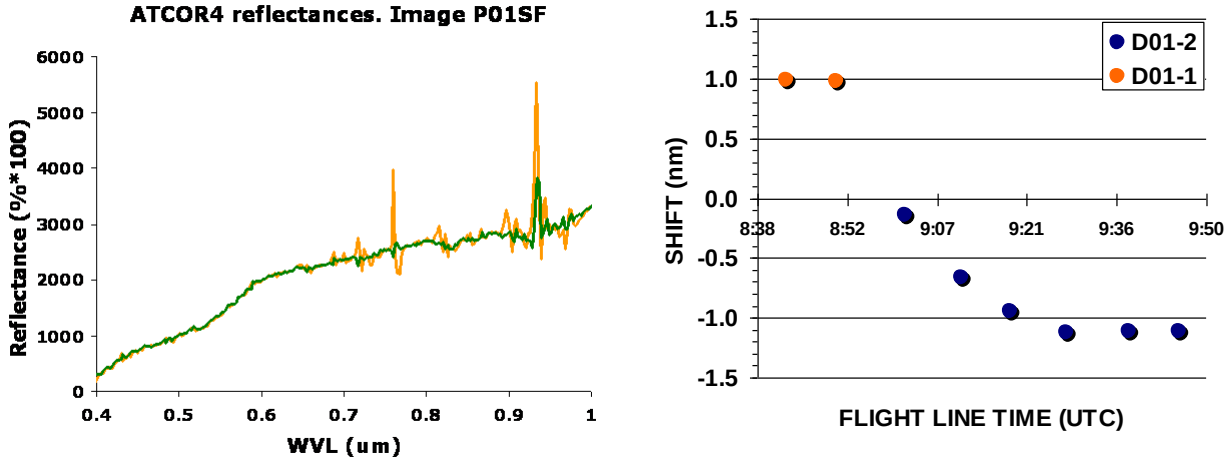

Figure 3, Left: CASI reflectance spectra (2.4 nm resolution) derived from nominal Ls (orange) and Ls corrected using the INTA procedure described in the text (green). Right: band center shift detected by the INTA procedure during a flight session (REFLEX campaign, 2012-07-25). The session started with D01-1, at 1000 m altitude, and was followed by the 2000 m flight D01-2.

Cartographic accuracy

On flat terrain, the main contributor to the error budget is the uncertainty in the boresight angles. Overall, and as confirmed during dedicated studies, we have estimated that the usual absolute geolocation error is isotropic and below 1 pixel. In rugged terrain, DEM resolution and accuracy becomes a major contributor to the error budget.

To check the actual absolute cartographic accuracy in a specific image, the usual way is to collect ground control points (GCPs). However, the selection of GCPs is difficult, when the original sample is highly rectangular (along-track size significantly larger than across-track size), because the original measurements have to "struggle" to fit in the required square grid, and the eventual statistical figure obtained is not related with the actual geometry of each sample but with the pixel size selected for the output grid. In such cases, it could be better to estimate error from the theoretical error budget modulated with actual figures of navigation uncertainty.

FUTURE WORK

The processing chain described in the previous sections is fully operational, and it is planned to maintain its basic elements in the near future with only minor modifications. Future work will be aimed at extending its capabilities, and three topics are currently considered in this sense:

- spectral stray light estimation and correction.
- reporting of actual geolocation error budget per campaign in the metadata files, in order to evaluate cartographic accuracy without using resampled data.
- implementation of specific procedures for the estimation of reflectance in forest canopies (a frequent target of hyperspectral remote sensing studies), where the observation and illumination angles are not defined by the terrain model and where the number of shadowed pixels is significant, but they cannot be detected with simple methods.

REFERENCES

1 de Miguel E, A Fernández-Renau, E Prado, M Jiménez, Ó G de la Cámara, C Linés, J A Gómez, A I Martín & F Muñoz, 2014. A review of INTA AHS PAF. EARSeL eProceedings, 13(1): 20-29

2 Hutton J, A Ip, T Bourke, B Scherzinger, N Gopaul & P Canter, 2008. Tight integration of GNSS post-processed Virtual Reference Station with inertial data for increased accuracy and productivity of airborne mapping. The International Archives of the Photogrammetry, Remote Sensing and Spatial Information Sciences, 37(B5): 829-834

3 Holzwarth S, R Müller & C Simon, 2005. Determination and monitoring of boresight misalignment angles during the hymap campaigns HYEUROPE 2003 and HYEUROPE 2004. In: 4th EARSeL Workshop on Imaging Spectroscopy - New Quality in Environmental Studies, edited by B Zagajewski, M Sobczak & M Wrzesień (EARSeL and Warsaw University, Warsaw)

4 González Lagos M, E de Miguel Llanes, M Jiménez Michavila & E Prado Ortega, 2012. Pérdida y redundancia de información en imágenes aeroportadas georreferenciadas sobre zonas de montaña. In: XV Congreso Nacional de Tecnologías de la Información Geográfica, edited by J Martínez Vega & P Martín Isabel (CSIC, Madrid). 563-572

5 Richter R & D Schläpfer, 2002. Geo-atmospheric processing of airborne imaging spectrometry data. Part 2: Atmospheric/Topographic correction. International Journal of Remote Sensing, 23(13): 2631-2649

6 Schaepman-Strub G, M E Schaepman, T H Painter, S Dangel & J V Martonchik, 2006. Reflectance quantities in optical remote sensing - definitions and case studies. Remote Sensing of Environment, 103: 27-42

7 Holzwarth, S, M Bachmann, M Freer & M Hofmann, 2011. Standards for airborne hyperspectral image data. In: Proceedings of the EARSeL 7th SIG-Imaging Spectroscopy Workshop, 7 pp.

8 Guanter L, R Richter & J Moreno, 2006. Spectral calibration of hyperspectral imagery using atmospheric absorption features. Applied Optics, 45: 2360-2370

9 Martinez L, F Pérez, R Arbiol & A Tarda, 2010. Radiometric characterization of a VNIR hyperspectral imaging system for accurate atmospheric correction. In: 2nd Workshop on Hyperspectral Image and Signal Processing - Evolution in Remote Sensing (WHISPERS), (Reykjavik, Iceland)

10 Gao B C, M J Montes & C O Davis, 2004. Refinement of wavelength calibrations of hyperspectral imaging data using a spectrum-matching technique. Remote Sensing of Environment, 90: 424-433